Struct Multidisc Optim (2011) 44:471–481
DOI 10.1007/s00158-011-0650-y

RESEARCH PAPER

Topology optimization using B-spline finite elements

Ashok V. Kumar · Anand Parthasarathy

Received: 14 May 2010 / Revised: 1 February 2011 / Accepted: 20 March 2011 / Published online: 7 May 2011

Abstract Topology optimization algorithms using traditional elements often do not yield well-defined smooth boundaries. The computed optimal material distributions have problems such as "checkerboard" pattern formation unless special techniques, such as filtering, are used to suppress them. Even when the contours of a continuous density function are defined as the boundary, the solution can still have shape irregularities. The ability of B-spline elements to mitigate these problems are studied here by using these elements to both represent the density function as well as to perform structural analysis. B-spline elements can represent the density function and the displacement field as tangent and curvature continuous functions. Therefore, stresses and strains computed using these elements is continuous between elements. Furthermore, fewer quadratic and cubic B-spline elements are needed to obtain acceptable solutions. Results obtained by B-spline elements are compared with traditional elements using compliance as objective function augmented by a density smoothing scheme that eliminates mesh dependence of the solutions while promoting smoother shapes.

Keywords Topology optimization · B-spline finite elements · Compliance minimization · Density smoothing

1 Introduction

Topology optimization is traditionally viewed as an approach that optimizes the material layout or distribution within a given design space with known loads and boundary conditions. By treating nodal or element density (or porosity) as design variables, the final optimal material distribution computed yields an optimal conceptual design for structures even if the final shape obtained is not smooth and has various shape irregularities. Topology optimization has now been applied to a variety of applications and has evolved into powerful conceptual design tool for structural design. Even so, it is desirable that well-defined, smooth boundaries can be obtained for optimal geometry without having to use an extremely dense mesh for analysis and optimization.

Several methods have been developed for topology optimization over the last two decades. The earliest approach for topology optimization involved removing elements with low stresses. However, such an approach has been shown to be ill-posed (Kohn and Strang 1986) and homogenization was suggested as a method for relaxing the "0–1 dichotomy" between regions with and without material. Therefore, homogenization based methods that treat porosity of elements as design variables were proposed and used for topology optimization (Bendsøe and Kikuchi 1988; Bendsøe et al. 1992). The homogenization method is used to compute the relation between material properties and porosity. The computed relation depends on the microstructure assumed for the porous material. Alternatively, several authors have used artificially designed material property–density relation (Bendsøe 1989; Rozvany et al. 1992, 1994; Kumar and Gossard 1992, 1996; Bendsøe and Sigmund 2003). The material property versus density relation is designed such that during the optimization process the density is driven to the upper limit (or unity) in regions that need material and driven to zero inside holes by penalizing intermediate values of density. This approach, often referred to as SIMP (Solid Isotropic Material with Penalization)

A. V. Kumar (✉) · A. Parthasarathy
Mechanical and Aerospace Engineering, University of Florida, Gainesville, FL 32611, USA
e-mail: akumar@ufl.edu

(Rozvany et al. 1992), typically assumes that the Young's modulus is proportional to some power of density. Other approaches such as genetic algorithms (Chapman et al. 1994; Madeira et al. 2010; Tai and Prasad 2007) and Evolutionary Structural Optimization (ESO) (Xie and Steven 1993; Chu et al. 1997) have also been developed for topology optimization. Some of the problems with the ESO approach have been pointed out by Zhou and Rozvany (2001). Genetic algorithm and ESO use a 0–1 approach for geometry representation where the elements are either on or off depending upon whether material is needed in a region. The 0–1 approach results in jagged boundaries. Even approaches that use density or porosity of the elements as design variables cannot represent smooth boundaries if they assume that the density is constant within each element because the contours of the density function are not continuous. In addition, early studies found that checker board patterns (Diaz and Sigmund 1995; Jog and Haber 1996; Bendsøe and Sigmund 2003) are obtained in some regions of the optimal design. To represent smoother boundaries, nodal values of density have been used as the design variables so that the density can be interpolated within elements to obtain a continuous density function (Kumar and Gossard 1996). This approach has since been used in conjunction with homogenization method and named continuous approximation of material distribution (CAMD) by Matsui and Terada (2004). If the density function is continuously interpolated, the contours of this function can represent a continuous boundary. Even though this approach, naturally excludes checkerboard patterns, other shape irregularities such as "islanding" and "layering" have been observed (Rahmatalla and Swan 2004). Contours or level sets of functions are used to represent boundaries in the level set method which solves the Hamilton-Jacobi differential equations to simulate moving boundaries. This method has been applied to topology optimization by several authors (Sethian and Wiegmann 2000; Wang et al. 2003; Xing et al. 2010). This approach yields smooth boundaries but the results are highly dependent on the initial level set assigned because inner boundaries are not automatically created. Techniques for introducing inner fronts have been proposed (Park and Youn 2008) to overcome this problem.

One way to avoid shape irregularities using the traditional SIMP approach is to use better quality elements. This is based on the understanding that fundamentally checkerboard patterns and other shape irregularities are a result of inadequate or poor numerical modeling. Topology optimization using honeycomb meshes whose elements use Wachspress shape functions were studied by Talischi et al. (2009) and shown to yield checkerboard-free designs. Higher order elements and mixed finite elements (Bruggi 2008) have also been studied and shown to be beneficial in suppressing checkerboard patterns.

In this paper, shape irregularities are avoided by using B-spline elements which are able to represent the density as tangent continuous and even curvature continuous functions so that the contours of the density function, which are the boundaries of the shape, also have similar continuity and smoothness. B-spline approximation schemes were originally developed for fitting smooth curves or surfaces to data. Their main application has been for geometric modeling and graphics where they have proved to be an intuitive and interactive shape design tool. B-splines approximations are created piece-wise over patches or elements in such a way that the resultant curves or surfaces are tangent (and curvature) continuous if quadratic (or cubic) splines are used. Unlike interpolation schemes, B-spline approximations do not pass through the data or nodal values that it is approximating. As a result the nodal value is not equal to the value of the approximating function at the node. This poses a challenge in applying boundary conditions using traditional approaches used in FEM. In addition, B-spline approximations are hard to construct for unstructured mesh with arbitrary shaped quadrilateral elements. For these reasons, B-spline approximations have not been used in traditional finite element method. In the Implicit Boundary Finite Element Method (IBFEM) (Kumar et al. 2008; Burla and Kumar 2008), a structured mesh, which has uniform, regular shaped elements, is used for the analysis and special solution structures are constructed to impose boundary conditions. This allows B-spline elements to be used even for relatively complex domain geometry. This approach is used in this paper for the analysis as well as for representing the density function whose contour defines the boundary of the structure. Recently, there has been significant research effort using isogeometric method for shape optimization (Wall et al. 2008; Cho and Ha 2009) as well as for shape and topology optimization (Seo et al. 2010). Isogeometric method uses B-spline or NURBS basis functions for both representing the geometry as well as the analysis solution. It should be noted that in the approach presented here, even though B-spline basis is used for representing the density function, it is the contours or level sets of this density function that represents the boundaries.

When the topology design problem is stated as a material distribution problem, in addition to shape irregularities, mesh dependence is another type of the numerical instability that has been observed. Traditional approaches do not eliminate mesh dependence unless additional techniques are used (Sigmund and Peterson 1998; Bendsøe and Sigmund 2003), such as using perimeter constraints or filters. In this paper, a density smoothing scheme is introduced to obtain mesh independent solutions. In Section 2, a brief summary

of B-spline elements and their shape functions are provided. The optimization problem is described in Section 3 and several 2D examples are provided in Section 4 that compare results obtained using traditional elements and B-spline elements. Finally, Section 5 provides some conclusions and discussions.

2 B-spline elements

B-spline functions can be used to approximate a given set of points with smooth polynomial functions. In traditional applications of B-splines such as geometric modeling and graphics, it is convenient to express B-spline basis function and approximations using recursive formulae (Farin 2002). For the finite element method, it is preferred that polynomial shape functions are derived for the B-spline elements so that the approximation within each element can be expressed as a weighted sum of nodal values. An isoparametric formulation of these elements can be implemented by deriving shape functions for a square element in parametric space (Burla and Kumar 2008). For each element in the grid an independent parameter space is defined as in traditional isoparametric finite elements. In the parametric space, the element domain is [−1,1] along each dimension. Shape functions that correspond to uniform B-splines can be derived for the one-dimensional case using the conditions of continuity of the approximation at the nodes. These can then easily be extended to higher dimensions if we assume that the elements in the mesh are rectangular and uniform or in other words, if the mesh is structured.

When displacements are represented using B-spline approximations, the nodal values do not correspond to the actual displacement at the node since B-splines do not interpolate the nodal values. Figure 1 shows a cubic B-spline approximation which is C^2 continuous. As shown in the figure, unlike the traditional finite element interpolation, the B-spline approximation does not pass through the nodal values.

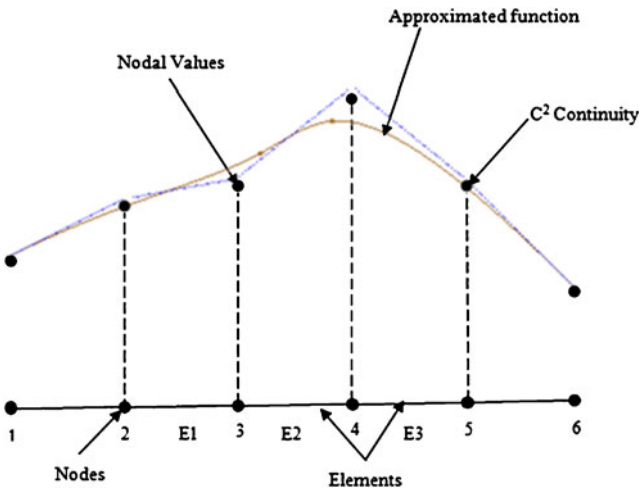

Fig. 1 Function approximated by 1D cubic B-spline

The element E2 is defined between vertex nodes 3 and 4, but the approximation defined over E2 (referred to as its span) is controlled by the nodal values at four nodes (node 2 to node 5) which are its support nodes. The polynomial expressions for the basis functions can be derived using the continuity requirements between adjacent elements. A k^{th} order B-spline has $k+1$ support nodes with some of them lying outside the element. The basis functions for the 1D quadratic B-spline and cubic B-spline can be derived as follows (Burla and Kumar 2008).

Quadratic B-spline element:

$$N_1 = \frac{1}{8}\left(1 - 2r + r^2\right) \tag{1}$$

$$N_2 = \frac{1}{8}\left(6 - 2r^2\right) \tag{2}$$

$$N_3 = \frac{1}{8}\left(1 + 2r + r^2\right) \tag{3}$$

Cubic B-spline element:

$$N_1 = \frac{1}{48}\left(1 - 3r + 3r^2 - r^3\right) \tag{4}$$

$$N_2 = \frac{1}{48}\left(23 - 15r - 3r^2 + 3r^3\right) \tag{5}$$

$$N_3 = \frac{1}{48}\left(23 + 15r - 3r^2 - 3r^3\right) \tag{6}$$

$$N_4 = \frac{1}{48}\left(1 + 3r + 3r^2 + r^3\right) \tag{7}$$

These basis functions form a partition of unity, which is an important property for convergence of the approximate solutions. The approximation within an element is a weighted sum of these shape functions that can be expressed as,

$$u(r) = \sum_{i=0}^{n} u_i N_i(r) \tag{8}$$

where, the weights u_i are referred as nodal values in this paper even though in traditional geometric modeling literature they are called control points. As the shape function N_i does not have unit value at node i, the value of the approximation at that node is not equal to u_i.

B-spline basis functions have compact support and lead to banded stiffness matrices. However, since some of the

nodes of the element are outside the element it has a wider support than traditional elements. Figure 2 shows 2D quadratic and cubic B-spline elements and their support nodes. The 2D basis functions for the bi-quadratic B-spline element can be constructed using the product of 1D quadratic basis functions. In this case, there are 9 support nodes and the element is referred to here as B-spline9N element. Similarly, 2D cubic B-spline elements are constructed as a product of 1D cubic B-spline functions. In this case, there are 16 support nodes and the element is referred to here as B-spline16N.

The shape functions of the quadratic and cubic B-spline elements can be expressed succinctly as:

$$N^{quad}_{3(j-1)+i}(r,s) = N_i(r)N_j(s), \qquad i,j = 1,\ldots,3$$
$$N^{cubic}_{4(j-1)+i}(r,s) = N_i(r)N_j(s), \qquad i,j = 1,\ldots,4 \tag{9}$$

The quadratic and higher order B-spline elements yield continuous stresses and strains between elements. If the density function for topology optimization is also approximated using the B-spline shape functions then the resultant boundaries will be tangent continuous for quadratic and curvature continuous for cubic B-splines.

When the value of the approximation at the nodes is not equal to the nodal value, traditional methods for applying displacement boundary conditions do not work. For example, the value of the displacement along a boundary cannot be set equal to a specified value by assigning the nodal values equal to the specified value. In this paper, the implicit boundary method (Burla and Kumar 2008) is used to assign boundary conditions. This method can impose boundary conditions even when the boundary does not have any nodes on it. This approach is briefly summarized below.

In the implicit boundary method, a trial solution structure for the displacement field is constructed as

$$\{\mathbf{u}\} = [\mathbf{D}]\{\mathbf{u}^g\} + \{\mathbf{u}^a\} = \{\mathbf{u}^s\} + \{\mathbf{u}^a\} \tag{10}$$

In this solution structure, $\{\mathbf{u}^g\}$ is a grid variable represented by piece-wise approximation using B-spline shape functions over the grid, and $\{\mathbf{u}^a\}$ is the boundary value function which is a vector field constructed such that it takes on the prescribed values of displacements at boundaries. $[\mathbf{D}] = diag(D_i, .., D_{n_d})$ is a diagonal matrix whose components D_i are Dirichlet functions that vanish on boundaries on which the i^{th} component of displacement is specified, n_d is the dimension of the problem.

In the implicit boundary method, approximate step functions are used as Dirichlet functions. These functions can be constructed using any type of implicit equation of the boundary. If the boundary condition is specified on a boundary whose implicit equation is $\Phi(\mathbf{x}) = 0$ then the step function for that boundary can be defined as

$$D(\Phi) = \begin{cases} 0 & \Phi \le 0 \\ 1 - \left(1 - \dfrac{\Phi}{\delta}\right)^2 & 0 \le \Phi \le \delta \\ 1 & \Phi \ge \delta \end{cases} \tag{11}$$

This function is an approximate step function that tends to the Heaviside step function in the limit as $\delta \to 0$ and has a value of zero on the boundary. Moreover, for use as an Dirichlet function, $D(\Phi)$ is constructed to have non-zero gradient at $\Phi = 0$. At $\Phi = \delta$ this function has C^1 continuity. In this paper, the step function approximation of D with $\delta \to 0$ is used with values of $\delta \approx 10^{-5}$ or smaller. The solution structure in (10), can be substituted into the principle of virtual work to derive the element stiffness matrices and load vectors (Burla and Kumar 2008).

3 Optimization problem statement

Minimization of the compliance of a structure is a traditionally used objective function for topology optimization

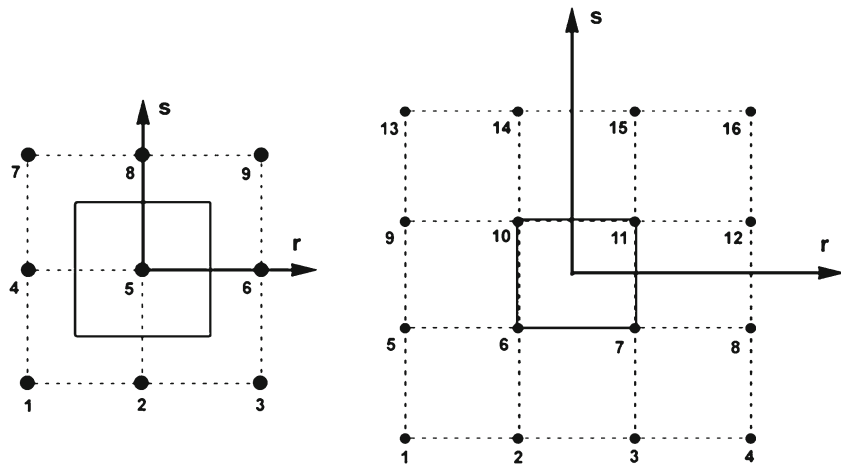

Fig. 2 2D quadratic and 2D cubic B-spline elements

and has been used with almost all the topology optimization methods. Therefore, we have used compliance minimization problem to demonstrate the use of B-spline elements for topology optimization. Minimization of the overall compliance results in effectively maximizing the stiffness of the structure. In this paper, this objective function is augmented with a term that penalizes the square of the gradient of density to smooth the density function in order to eliminate mesh dependence of the solution. Several other techniques for eliminating mesh dependence have been used in past work, such as adding a constraint on perimeter, restricting gradients or filtering the density or sensitivity (Sigmund and Peterson 1998; Bendsøe and Sigmund 2003). In this paper, instead of adding a constraint on the perimeter, the density function is smoothened by minimizing the square of the gradient of density integrated over the volume to create a multi-objective optimization problem. Smoothing the density function prevents the appearance of large number of holes as in a porous material, which is the theoretical optimum. This effectively eliminates the mesh dependence which arises mainly due to the ability of higher density meshes to represent finer and finer pattern of holes. The minimization problem can be stated as:

$$\text{Minimize} : \prod = \int_{\Gamma} \{f\}^T \{u\} d\Gamma + w \int_{V} (\nabla\phi)^2 dV \tag{12}$$

$$\text{subject to}, M(\phi) = \int_{\Omega} \phi \, d\Omega \leq M_0 \tag{13}$$

$$\int_{\Omega_0} \{\delta\varepsilon\}^T [C(\phi)] \{\varepsilon\} d\Omega = \int_{\Gamma} \{\delta u\}^T \{f\} d\Gamma \tag{14}$$

$$\phi_{th} \leq \phi \leq 1 \tag{15}$$

In (12), the first term is the compliance and the second term is a weighted penalty on square of the gradient of density where w is the weighting factor referred to here as the *penalty factor*. The second term in objective function is a penalty on the magnitude of the gradient of density as explained below and is computed as follows

$$P = \int_{V} (\nabla\phi)^2 dV = \sum_{e=1}^{\mathrm{n_e}} \int_{V_e} \left(\sum_{j=1}^{npe} \phi_j \frac{\partial N_j}{\partial x_i} \right)^2 dV \tag{16}$$

Here ϕ_j is the nodal value of the density, $\frac{\partial N_j}{\partial x_i}$ is the gradient of the nodal shape functions, *npe* is the number of nodes per element and n_e is the number of elements in the mesh. The second term in the objective function penalizes the gradient of density and it also indirectly penalizes the perimeter since the magnitude of the gradient of the density is maximum at boundaries where the density transitions from 0 to 1. By penalizing the magnitude of the gradient, the density function is smoother and has less wriggles which smoothens the boundaries and minimizes the perimeter also. This approach is therefore similar to past work where constraint on perimeter has been shown to be an effective way of removing mesh dependence of the solution.

The current design or the geometry of domain is defined as the region within the original feasible domain, in which the density function has a value greater than a threshold value of $\phi = 0.5$. The nodal values of the density function are the design variables. The traditional SIMP approach is used to define the material property–density relation as

$$E = \phi(x, y)^p E_0 \tag{17}$$

This approach (with $p > 1$) automatically penalizes intermediate density values forcing it to be either 0 or 1. The optimization algorithm would decrease the densities in those regions where the material is underutilized resulting in new holes or shrinking existing boundaries inwards. A sequential optimization algorithm using logarithmic barriers (Kumar 2000) was used here which requires the evaluation of the gradient of the objective function. The gradient of compliance of the structure is given by,

$$\frac{\partial L(\phi)}{\partial \phi_i} = \{f\}^T \frac{\partial \{u\}}{\partial \phi_i} = -\{u\}^T \frac{\partial [K]}{\partial \phi_i} \{u\} \tag{18}$$

The sensitivity of the smoothing term with respect to the nodal density can be computed as given below,

$$\frac{\partial P}{\partial \phi_j} = \int_{V} 2(\nabla\phi) \cdot \frac{\partial(\nabla\phi)}{\partial \phi_j} \, dV \tag{19}$$

4 Results

Several examples are studied here to compare results obtained using the traditional 4 node bilinear quadrilateral elements (Quad4N) with results obtained using quadratic (B-spline9N) and cubic B-spline (B-spline16N) elements.

4.1 L-shaped structure

In this example, compliance minimization in an L-shaped feasible region is used to study the nature of the optimal shapes obtained using B-spline elements. Figure 3 shows the L-shaped region with dimensions and the initial mesh used for the plane stress model for topology optimization. A point load of 200 N is applied along the right edge and the domain is constrained along the top edge. The material of the domain is assumed to be steel with a modulus of

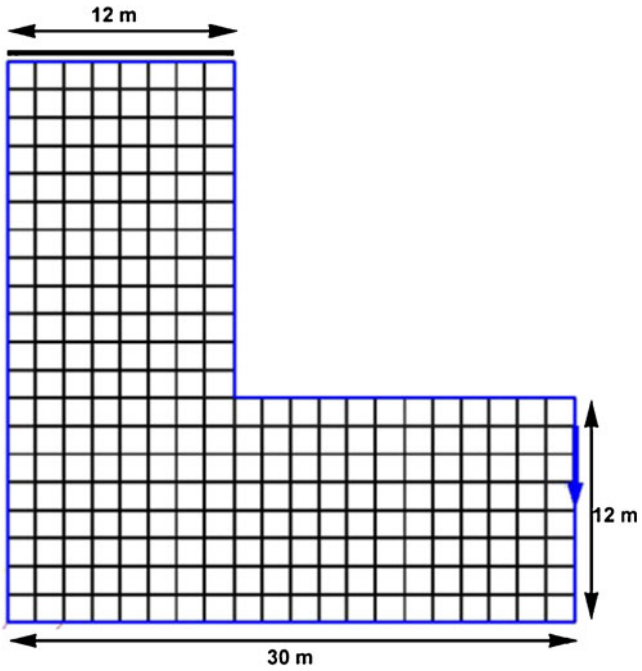

Fig. 3 Plane stress model of the L-shaped structure

elasticity equal to 200 GPa and the Poisson's ratio of 0.3. A mesh consisting of 20 elements along the longest edges is used. Typically much denser mesh is used for topology optimization. A sparse mesh is used here first to demonstrate that reasonable results can be obtained even with this mesh using B-spline elements.

Figure 4 shows the topology designs computed using nodal values as design variables and SIMP method with the penalty parameter p = 4 and the allowable mass equal to 0.5 of the feasible domain. Optimal shape obtained without penalizing gradient of density is shown in Fig. 4a–d for bilinear 4 node (Quad4N), biquadratic 9 node (Quad9N), B-spline 9 node (B-spline9N) and B-spline 16 node (B-spline16N) elements respectively. Figure 4e–h shows results obtained using these same elements when the objective function includes a penalty on gradient of density applied with a penalty factor of 10^{-7}. In all these examples, the same number of elements was used as shown in Fig. 3 but the number of nodes is significantly higher for quadratic Lagrange elements. The optimal shape obtained for Quad9N is different and without penalization leads to a pattern of holes.

It can be observed that using B-spline elements smoother shapes are obtained when compared with the bilinear and biquadratic Lagrange elements. It is evident that the results obtained differ somewhat with the type of the element used. However, when the penalty on gradient of density is applied (Fig. 4e–h), the results tend to converge towards the same shape with the B-spline elements yielding slightly smoother shapes. For 16 node cubic B-spline elements, the optimal

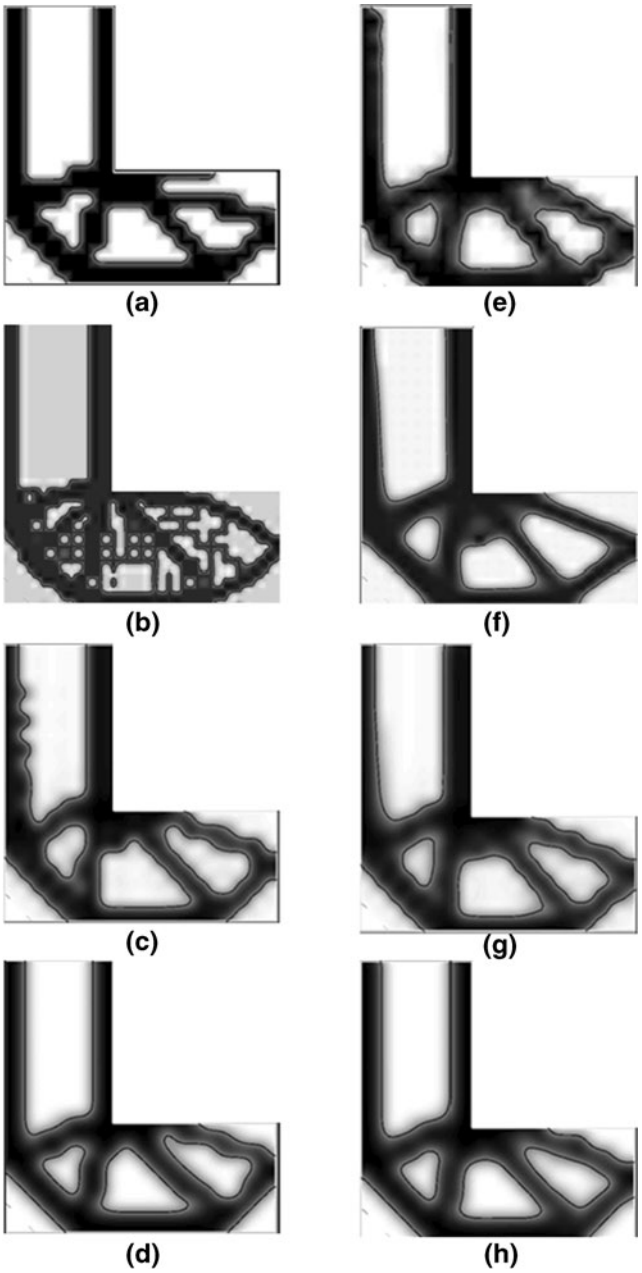

Fig. 4 Topology design using a 20 × 20 mesh **a** Quad4N, **b** Quad9N, **c** B-spline9N, **d** B-spline16N, **e** Quad4N with smoothing, **f** Quad9N with smoothing, **g** B-spline9N with smoothing, **h** B-spline16N with smoothing

shape and topology is similar with and without the penalty on gradient of density which suggests that the B-spline16N element has a built-in smoothing mechanism. This may be due to the fact the 16 node cubic elements have a larger support compared to the other elements. Since the density within the element is influenced by nodes that are outside the element this inherently has a smoothing effect similar to density filtering schemes used for eliminating mesh dependence where the element density is set equal to the average of the densities of neighboring elements.

To study the mesh dependence of the solution, a much more refined mesh is used next to check if the topologies obtained would be different from the topologies obtained using a sparse mesh. A refined mesh that has 70 elements along the longest edge is used for the L-shaped region to obtain the results in Fig. 5. Again, the penalty parameter of $p = 4$ and the allowable mass fraction of 0.5 is used. Figure 5a–d shows results obtained without smoothing of the density. Clearly, the results are not the same as those obtained previously with the sparser mesh. Moreover, for the same mesh size, the results obtained using different element types are not the same. Smaller holes appear in the results obtained using the bilinear Quad4N elements and a fine patch work of holes are obtained with the Quad9N elements indicating that a porous material is the optimal. In contrast, well-defined non-porous designs are obtained with the B-spline elements. This again is consistent with the idea that there is a larger length scale associated with B-spline elements due to their wider support. But the solution for B-splines with finer mesh is not the same as the solution with sparser mesh because the length scale is related to the element size. Therefore, a finer mesh allows smaller holes to be represented.

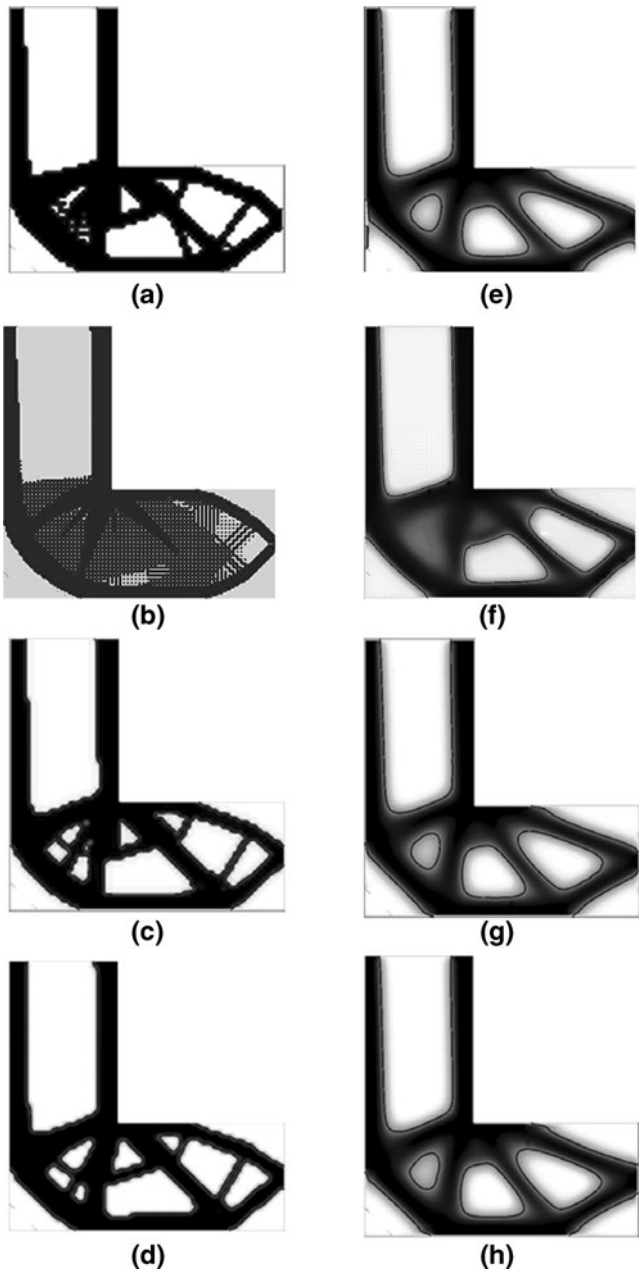

Fig. 5 Topology design using a 70×70 mesh **a** Quad4N, **b** Quad9N, **c** B-spline9N, **d** B-spline16N, **e** Quad4N with smoothing, **f** Quad9N with smoothing, **g** B-spline9N with smoothing, **h** B-spline16N with smoothing

Figure 5e–h show the designs obtained with the smoothing of density for the same four types of elements using a penalty factor of 10^{-7}. It is clear that the penalty on the gradient of density (or smoothing) eliminates both the dependence on mesh density and the element type used. The results obtained using all four element types are the same when smoothing is applied and the topology is similar to the results obtained using the sparser mesh in Fig. 4.

In all the four models, the number of elements is the same but the number of nodes is not the same. For the examples shown in Fig. 4 the number of elements is 256 and the number of nodes for each element type is listed in Table 1. The nodes used for density representation and for displacement approximation during analysis are the same. Only the biquadratic Quad9N element uses a significantly higher number of nodes per element. Unlike the traditional quadratic element the B-spline elements have external nodes that are shared with neighboring elements (Burla and Kumar 2008). As a result the number of nodes in the mesh is not much higher than Quad4N. As can be seen from Fig. 2, the B-spline16N element mesh and the Quad4N mesh will have the same nodes except along the boundaries where the B-spline elements will have some extra external nodes.

In both Figs. 4 and 5, the density is plotted with black where density is one and white where density is zero and with grayscales for values in between. In addition, the contour or level set corresponding to density equal to half is plotted in black color. When a dense mesh is used the

Table 1 Number of nodes used for each element type

Element type	Number of nodes	Node per element
Bilinear Q4	297	1.16
Biquadratic Q9	1,105	4.32
B-spline 9N	340	1.33
B-spline 16N	385	1.50

density transitions from zero to one sharply, giving us well-defined boundaries. When smoothing is used or B-spline elements with low mesh density is used the density cannot sharply transition to zero at the boundary. In these cases due to penalty on magnitude of density gradient or due to the smoothing effect of B-splines, the transition of density from zero to one happens smoothly over a wider region. The contour plot of density equal to half allows us to extract a smooth well-defined boundary in these cases.

Convergence plots are shown in Fig. 6 for the bilinear Quad4N, B-spline9N and B-spline16N elements, where, the compliance of the structure is plotted as a function of the number of iterations. The comparison between these three elements is reasonable since the number of nodes is very similar. These convergence plots indicate that the rate of convergence is similar for these three element types studied here.

Table 2 shows the values of the compliance of the final optimal structure along with the total number of iterations required for convergence. There is no significant improvement in convergence upon using higher order elements. While the optimal shapes are smoother and better defined for higher order elements, the total computation time is of course higher.

A plot of compliance versus number of nodes in the model is shown for different types of elements in Fig. 7. The final compliance obtained for the optimal structure using B-spline9N and B-spline16N elements are slightly higher than the compliance obtained using the bilinear Quad4N elements. This is related to the fact that B-spline elements yield smoother shapes with fewer holes and shape irregularities. Bilinear Quad4N elements allow shapes that are non-smooth or have irregularities and such shapes have lower compliance (or higher stiffness) but are unacceptable from a design perspective.

Table 2 Compliance convergence results for various elements

Element type	Compliance	Iterations to converge
Bilinear Q4	3.619E-5	128
B-spline 9N	3.6435E-5	127
B-spline 16N	3.7138E-5	105

The effect of smoothing using penalty on the gradient of density is shown in Fig. 8. The plot shows the compliance values for the optimal structure obtained using bilinear Quad4N elements only. Lower values of compliance can be achieved when smoothing is not imposed. The penalty favors designs with fewer holes and also has the effect of eliminating the wriggles on the boundaries. Therefore, the search for the optimal design occurs in a more restricted design space. The difference in the values of compliance with and without penalization is less than 10% and is therefore not very significant.

4.2 Cantilever structure

A short cantilever beam-like structure is considered here to demonstrate the natural smoothing and checkerboard suppression provided by B-spline elements. The plane stress model of the cantilever beam along with the loads and boundary conditions is shown in the Fig. 9a. The topology optimization of the structure for minimum compliance with a constraint on the weight of the structure is performed. The rectangular feasible domain of dimensions 80×20 m is subjected to a point load of 100 N applied at the midpoint of the right edge. The structure is constrained along the left edge of the domain. The material of the structure is assumed to be steel with the modulus of elasticity equal to 200 GPa and

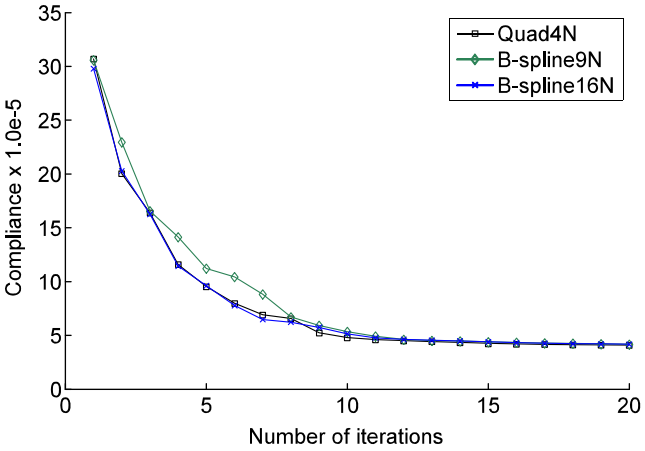

Fig. 6 Compliance convergence plot for a mesh size of 70×70 **a** Quad4N element, **b** B-spline9N element, **c** B-spline16N element

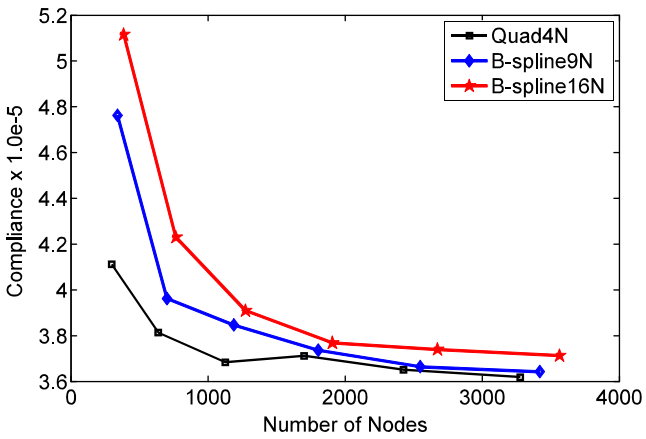

Fig. 7 Compliance plot for the L-shaped structure with varying mesh sizes for Quad4N, B-spline9N and B-spline16N elements

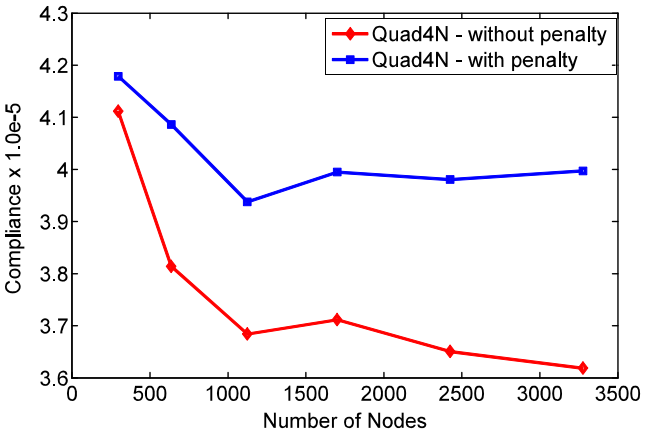

Fig. 8 Compliance plot for the L-shaped structure with varying mesh sizes for Quad4N elements with and without smoothing

the Poisson's ratio of 0.3. The domain has been discretized with a sparse mesh of 80 × 20.

The optimal topology results shown in Fig. 9 are computed using SIMP method with the penalty parameter p = 3 and allowable mass fraction of 0.6. Using the bilinear Quad4N elements, the computed optimal shape has islanding which is typically observed when nodal density is used as the variable and is analogous the checkerboard patterns seen when element densities are the variables.

Optimization using cubic B-spline (B-spline16N) elements converges to a well-defined shape with relatively smooth boundaries without using any filtering or checkerboard suppression schemes. The boundaries of the optimal shape shown in Fig. 9d have fewer wriggles compared to that obtained using the other two types of elements. Superior results are obtained using the cubic B-spline element not only because the density function is smoother and continuous but also because the solution to the plane-stress analysis is more accurate with B-spline elements since it uses cubic polynomial basis. As shown in the previous example, the results obtained using B-spline elements are not entirely mesh independent therefore it is likely that a different shape maybe obtained if a much higher density mesh is used. But the element size determines the smallest holes or links that can appear on the optimal design. Hence element size provides some control over the smallest features in the optimal shape in a manner similar to how filter radius provides a control on length scales in the optimal shape when density or sensitivity filters are used to avoid mesh dependence (Bendsøe and Sigmund 2003). By using

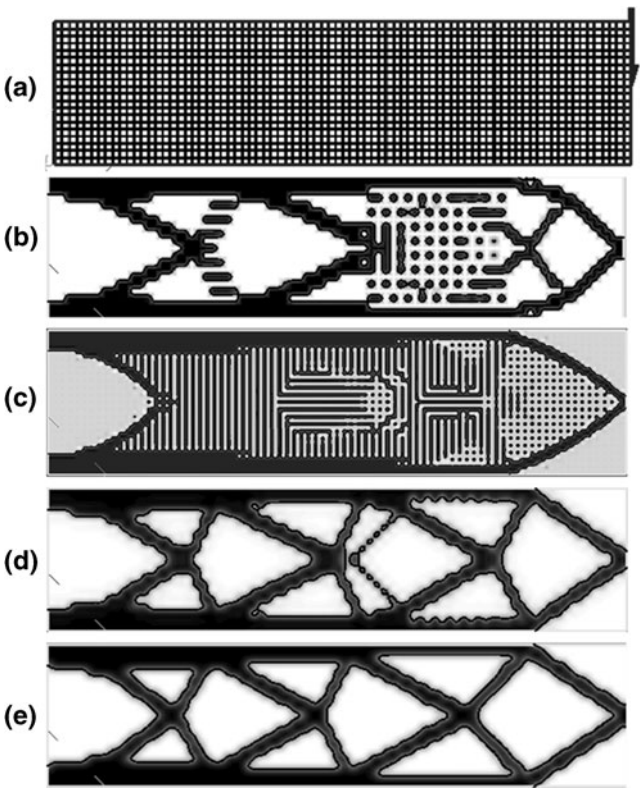

Fig. 9 Topology optimization results for the cantilever beam with a shear load using a 80 × 20 mesh and volume fraction of 0.6 **a** feasible domain, **b** Quad4N element, **c** Quad9N elements, **d** B-spline9N element, **e** B-spline16N element

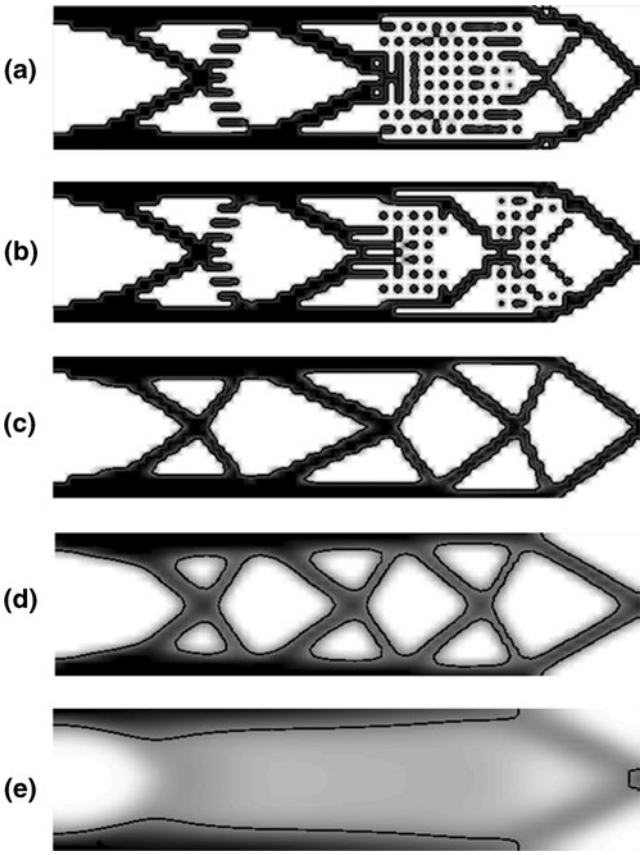

Fig. 10 Results with different weights for the smoothing term. Weight **a** w = 0, **b** w = 10^{-9}, **c** w = 10^{-8}, **d** w = 10^{-7}, **e** w = 10^{-6}

B-spline elements well-defined shape and topology can be obtained even with very sparse mesh so that element size can be selected approximately equal to the minimum feature size desired.

Smooth shapes can also be obtained using Quad4N by using penalty on the gradient of density. Figure 10 shows the effect of the penalty factor on the optimal results obtained using bilinear Quad4N elements.

It can be observed that when there is no smoothing applied ($w = 0$), islanding occurs similar to checkerboard patterns. With the increase in the penalty factor, smoother shapes are obtained that do not have any islands and the boundaries are progressively smoother. On the other hand, a very high value of the penalty factor results in a structure with grey areas and without any clear boundaries. Finding the appropriate value for the penalty factor is the main challenge in using the smoothing technique. In our implementation, the penalty factor was chosen based on the magnitude of the real objective function at the beginning of the optimization such that the penalty was not negligible nor does it dominate. It is interesting to note that for a penalty factor of 10^{-8}, the optimal shape obtained using Quad4N element (Fig. 10c) is very similar to that obtained using B-spline16N element without smoothing (Fig. 9d). Therefore, using B-splines with appropriate element size yields smooth shape and topologies without irregularities. These shapes can be further smoothed by using penalty on the density gradient if desired.

5 Conclusion

Topology optimization using B-spline elements was studied to compare it with traditional elements. The geometry was defined using contours of smooth and continuous density functions that also was represented using B-spline approximation. The nodal values of the density are treated as the design variables for topology optimization and the density varies continuously within the elements. Implicit boundary method was used for the application of boundary conditions and loads. Quadratic and cubic B-spline finite elements were used to obtain optimal shapes and the results compared with the traditional bilinear 4-node quadrilateral elements. With traditional elements, using different order of interpolation for density and displacement has been found to be beneficial. However, in this paper all the results presented have used the same order of interpolation or approximation for both density and displacement field. Results indicate that the B-spline elements naturally tend to suppress shape irregularities and using the same order approximation for density and displacement did not cause any instability. Even without smoothing or filtering, the optimal geometry obtained using B-splines have smooth well-defined boundaries even with relatively sparse mesh. However, the optimal results are mesh dependent unless a penalty on the gradient of density is imposed to smooth the density function. Without smoothing, the smallest feature that can appear in the optimal shape is roughly equal to the element size. The penalty on the gradient of density to achieve smoothing of the density function is similar to adding constraints on perimeter or gradients that has been used in the past (Bendsøe and Sigmund 2003) to eliminate mesh dependence. The implementation of a penalty on the gradient of density may be easier than implementing it as a perimeter or gradient constraint because it is difficult to estimate an appropriate value for such constraints. With the penalty approach, the penalty factor must be chosen carefully to ensure that the penalty term is not negligible or dominant compared to the real objective function. The smoothing achieved by adding this penalty to the objective function was found to effectively remove the mesh dependence of the solution. Further study is needed to explore the use of B-spline elements for other objectives such as designing compliant mechanisms. B-spline elements have been used for 3D structural analysis (Burla and Kumar 2008). Therefore, using these elements for topology optimization of 3D structures is expected to be straightforward. One of the challenges is to develop reliable algorithms for extracting the contours (or isosurface) of the density function to display the 3D results. The computational expense will of course be significantly higher for 3D applications.

Acknowledgements Kumar A.V. would like to acknowledge the financial support from Air Force Research Labs/RW for this research through contract FA8651-06-1-0001.

References

Bendsøe MP (1989) Optimal shape design as a material distribution problem. Struct Multidisc Optim 1:193–202

Bendsøe MP, Kikuchi N (1988) Generating optimal topologies in structural design using a homogenization method. Comput Methods Appl Mech Eng 71:197–224

Bendsøe MP, Sigmund O (2003) Topology optimization theory, methods and applications. Springer, New York

Bendsøe MP, Diaz A, Kikuchi N (1992) Topology and generalized layout optimization of elastic structures. In: Bendsøe MS (ed) Topology design of structures. Kluwer Academic Publishers, Dordrecht

Bruggi M (2008) On the solution of the checkerboard problem in mixed-FEM topology optimization. Comput Struct 86:1819–1829

Burla RK, Kumar AV (2008) Implicit boundary method for analysis using uniform B-spline and structured grid. Int J Numer Methods Eng 76:1993–2028

Chapman CD, Saitou K, Jakiela MJ (1994) Genetic algorithm as an approach to configuration and topology design. J Mech Des 116:1005–1012

Cho S, Ha SH (2009) Isogeometric shape design optimization: exact geometry and enhanced sensitivity. Struct Multidisc Optim 38:53–70

Chu DN, Xie YM, Hira A, Steven GP (1997) On various aspects of evolutionary structural optimization for problems with stiffness constraints. Finite Elem Anal Des 24:197–212

Diaz A, Sigmund O (1995) Checkerboard patterns in layout optimization. Struct Multidisc Optim 10:40–45

Farin G (2002) Curves and surfaces for CAGD: a practical guide. Morgan Kaufmann Publishers, San Francisco

Jog CS, Haber RB (1996) Stability of finite element models for distributed-parameter and topology design. Comput Methods Appl Mech Eng 130:203–226

Kohn RV, Strang G (1986) Optimal design and relaxation of variational problems. Comm Pure and Appl Math 39:113–137 (Part I), 139–182 (Part II) 333–350 (Part III)

Kumar AV (2000) A sequential optimization algorithm using logarithmic barriers: applications to structural optimization. J Mech Des 122(3):271–277

Kumar AV, Gossard DC (1992) Geometric modeling for shape and topology optimization. In: IFIP conference proceedings. Geometric Modeling for Product Realization

Kumar AV, Gossard DC (1996) Synthesis of optimal shape and topology of structures. J Mech Des Trans ASME 118:68–74

Kumar AV, Padmanabhan S, Burla RK (2008) Implicit boundary method for finite element analysis using non-conforming mesh or grid. Int J Numer Methods Eng 74:1421–1447

Madeira JFA, Pina HL, Rodrigues HC (2010) GA topology optimization using random keys for tree encoding of structures. Struct Multidisc Optim 40:227–240

Matsui K, Terada K (2004) Continuous approximation of material distribution for topology optimization. Int J Numer Methods Eng 59:1925–1944

Park KS, Youn SK (2008) Topology optimization of shell structures using adaptive inner-front (AIF) level set method. Struct Multidisc Optim 36:43–58

Rahmatalla SF, Swan CC (2004) A Q4/Q4 continuum structural topology optimization implementation. Struct Multidisc Optim 27:130–135

Rozvany GIN, Zhou M, Birker T (1992) Generalized shape optimization without homogenization. Struct Multidisc Optim 4: 250–254

Rozvany GIN, Zhou M, Sigmund O (1994) Topology optimization in structural design. In: Adeli H (ed) Advances in design optimization. Chapman and Hall, London

Seo YD, Kim HJ, Youn SK (2010) Shape optimization and its extension to topological design based on isogeometric analysis. Int J Solids Struct 47:1618–1640

Sethian JA, Wiegmann A (2000) Structural boundary design via level set and immersed interface methods. J Comput Phys 163(2): 489–528

Sigmund O, Peterson J (1998) Numerical instabilities in topology optimization: a survey on procedures dealing with checkerboards, mesh-dependencies and local minima. Struct Multidisc Optim 16:68–75

Tai K, Prasad J (2007) Target-matching test problem for multiobjective topology optimization using genetic algorithms. Struct Multidisc Optim 34:333–345

Talischi C, Paulino GH, Le CH (2009) Honeycomb Wachspress finite elements for structural topology optimization. Struct Multidisc Optim 37:569–583

Wall WA, Frenzel MA, Cryon C (2008) Isogeometric structural shape optimization. Comput Methods Appl Mech Eng 197:2976–2988

Wang MY, Wang XM, Guo DM (2003) A level set method for structural topology optimization. Comput Methods Appl Mech Eng 192:227–246

Xie YM, Steven GP (1993) A simple evolutionary procedure for structural optimization. Comput Struct 49:885–896

Xing X, Wei P, Wang MY (2010) A finite element based level set method for structural optimization. Int J Numer Methods Eng 82:805–842

Zhou M, Rozvany GIN (2001) On the validity of ESO type methods in topology optimization. Struct Multidisc Optim 21: 80–83